Published in final edited form as:
Nat Neurosci. 2021 May 01; 24(5): 658–666. doi:10.1038/s41593-021-00818-4.

Spinal astroglial cannabinoid receptors control pathological tremor

Eva Maria Meier Carlsen[1], **Sarah Falk**[1,2], **Urszula Skupio**[3], **Laurie Robin**[3], **Antonio C. Pagano Zottola**[3], **Giovanni Marsicano**[3], **Jean-François Perrier**[1,*]

[1]Department of Neuroscience, Faculty of Health and Medical Sciences, University of Copenhagen, Denmark

[2]Novo Nordisk Foundation Center for Basic Metabolic Research, Faculty of Health and Medical Sciences, University of Copenhagen, Denmark

[3]U1215 INSERM, NeuroCentre Magendie, University of Bordeaux, Bordeaux, France

Abstract

Cannabinoids reduce tremor associated with motor disorders induced by injuries and neurodegenerative disease. Here we show that this effect is mediated by cannabinoid receptors on astrocytes in the ventral horn of the spinal cord, where alternating limb movements are initiated. We first demonstrate that tremor is reduced in a mouse model of essential tremor after intrathecal injection of the cannabinoid analog WIN55,212-2. We investigate the underlying mechanism using electrophysiological recordings in spinal cord slices and show that endocannabinoids released from depolarized interneurons activate astrocytic cannabinoid receptors, causing an increase in intracellular Ca^{2+}, subsequent release of purines, and inhibition of excitatory neurotransmission. Finally, we show that the anti-tremor action of WIN55,212-2 in the spinal cords of mice is suppressed after knocking out CB_1 receptors in astrocytes. Our data suggest that cannabinoids reduce tremor via their action on spinal astrocytes.

Everyone experiences the involuntary, rhythmic, oscillatory movement of body parts that is known as tremor [1]. Physiological tremor is not a burden due to its modest amplitude. In contrast, pathological forms of tremor can be extremely disabling for patients [2], and can

*Corresponding author: Jean-François Perrier: perrier@sund.ku.dk, Department of Neuroscience, Faculty of Health and Medical Sciences, University of Copenhagen, Blegdamsvej 3, 2200 Copenhagen, Denmark.

The authors declare no competing interests.

Contributions:
EMC, JFP designed the project
EMC performed the electrophysiological and imaging experiments
SF and EMC performed the behavioral experiments
US, LR, APZ performed the validation of the transgenic model
GM, JFP supervised research
EMC, JFP wrote the paper
All authors approved the final version.

Reporting Summary
Further information on research design is available in the Nature Research Reporting Summary linked to this article.

Europe PMC Funders Author Manuscripts

arise during multiple sclerosis, stroke, neurodegenerative disorders, traumatic brain injury or essential tremor [3–6]. Patients who self-medicate report an improvement of tremor symptoms with cannabinoid-containing drugs, and the anti-tremor effect of cannabis has been confirmed in both clinical studies and an animal model of multiple sclerosis [7–11]. Δ^9-tetrahydrocannabinol (Δ^9-THC), the primary active compound in *Cannabis sativa*, acts as an agonist at G-protein-coupled cannabinoid (CB) receptors, which are ubiquitously expressed on axon terminals and astrocytes [12–18]. Under physiological conditions, CB receptors are activated by the endocannabinoids (eCBs) anandamide and 2-arachidonylglycerol (2-AG) [19], which are released upon demand by neuronal depolarization [12,13]. In the hippocampus, for example, depolarization of pyramidal neurons triggers eCB release, which causes activation of presynaptic CB_1 receptors and suppression of both inhibitory and excitatory neurotransmission [12,15]. In parallel, eCBs activate hippocampal astrocytes by increasing intracellular Ca^{2+} concentration, which triggers glutamate release that promotes synaptic transmission at neighboring synapses [15].

We investigate the role of eCBs in the ventral horn of the spinal cord; a region responsible for the organization of alternating limb movements [20]. In an animal model of essential tremor, we find that the CB receptor agonist WIN55,212-2 exerts a powerful anti-tremor effect when injected intrathecally. By combining electrophysiology, pharmacology and Ca^{2+} imaging in a slice preparation of the spinal cord, we discover that eCBs released from depolarized interneurons induce increases in intracellular Ca^{2+} in nearby astrocytes. In turn, these astrocytes release purines, which inhibit synaptic neurotransmission between excitatory axons and the depolarized interneurons. We also examine the behavioral consequences of eCB action in the spinal cord using a conditional mutant mouse line that lacks CB_1 receptors specifically in astrocytes. This reveals that spinal astrocytic CB_1 receptors are necessary for the anti-tremor effect of WIN55,212-2 in intact animals. Together, these data suggest that spinal astrocytes regulate tremor by purinergic modulation of synaptic transmission.

Results

Spinal cannabinoids receptors reduce tremor *in vivo*

To examine whether spinal eCB receptors are involved in tremor, we used a mouse model of essential tremor; the most common cause of tremor [6]. Intraperitoneal administration of harmaline into mice (Fig. 1a) [21,22] induces rhythmic burst-firing activity in the olivary nuclei that is transmitted to the spinal cord and eventually results in muscle tremor [23]. We tested the effect of activating spinal CB receptors in this model by intrathecal lumbar administration of the highly potent CB agonist WIN55,212-2. Thirty minutes after injection, tremor was strongly reduced in all animals tested (Fig. 1a,c). In contrast, injection of a vehicle had no effect on harmaline-induced tremor (Fig. 1b,c). When animals were pretreated with an intraperitoneal injection of the selective CB_1 antagonist AM281, WIN55,212-2 became as ineffective (Fig. 1d,f) as vehicle injection (Fig. 1e,f). This suggests that the anti-tremor effect of WIN55,212-2 is mediated by CB_1 receptors. We presume that WIN55,212-2 injected intrathecally acts specifically within the spinal cord, because diffusion of compounds in the central nervous system is inversely related to their molecular

weight [24], and intrathecally injected substances of lower molecular weight than WIN55,212-2 remain within the spinal cord for more than two hours [25]. Our results thus suggest that activation of CB_1 receptors on spinal cord neurons exerts a powerful anti-tremor effect.

Endocannabinoids released from spinal interneurons inhibit excitatory synaptic transmission

Given that centrally-originating tremor is transmitted to the spinal cord by excitatory pathways [26], we decided to investigate whether activation of spinal CB receptors modulates excitatory synaptic transmission. In other regions of the central nervous system, CB_1 receptors are activated by eCBs released from neurons following depolarization [27,28]. Subsequent binding of eCBs to presynaptic receptors transiently inhibits excitatory synaptic transmission; a phenomenon known as depolarization induced suppression of excitation (DSE) [13]. In a slice preparation of the spinal cord of juvenile mice, we found evidence for DSE when recording the amplitude of EPSCs in spinal ventral interneurons evoked by stimulation of excitatory axons before and after postsynaptic depolarization in 19 of 31 recordings (61%). DSE was accompanied by an increase in paired-pulse ratio (PPR; Fig. 2a,b,e) – a phenomenon of presynaptic origin in which the ratio between the second and first postsynaptic potential is increased [29]. This implied that DSE was also of presynaptic origin at this synapse. The degree of inhibition induced by neuronal depolarization was similar for synapses with high release probability (PPR<1; n=8) and low release probability (PPR>1; n=11; Mann Whitney test, $p = 0.55$). The selective CB_1 antagonist AM281 eliminated the effect of DSE on PPR (Fig. 2c,d,f-h). AM281 also unmasked an inhibition of the second potential following postsynaptic depolarization, which resulted in a modest decrease in PPR (Fig. 2f,h). This was not investigated further. Together, these results demonstrate that postsynaptic mobilization of eCBs from local interneurons underlies the inhibition of excitatory synaptic transmission that is associated with DSE in the ventral horn of the spinal cord. The data also reveal that PPR measurements are a good proxy for DSE.

Endocannabinoids inhibit synaptic transmission by inducing astrocytes to release purines

Previous evidence has shown that eCBs do not diffuse more than 20 μm from their release sites [12,27]. Interestingly, when we recorded two interneurons simultaneously, evoking EPSCs in one of them while testing the effect of depolarizing the other (Fig. 3a), we found the spatial extent of DSE was larger than this distance. We observed that a depolarizing pulse induced inhibition of EPSCs in 19 of the 29 pairs tested (66%), which was characterized by an AM281-sensitive increase in PPR (Fig. 3a-h). The degree of inhibition for synapses with high release probability (PPR<1; n=10) and low release probability (PPR>1; n=9) were similar (Mann Whitney test, $p = 0.97$). This form of DSE occurred between interneuron pairs whose somas were separated by up to 130 μm. Indeed, there was no correlation between distance and the degree of inhibition (Fig. 3i). These results clearly show that eCBs released from single neurons have a wider impact on synaptic transmission than expected from simple retrograde signaling, suggesting that the effect is broadcasted through an intermediary cell.

As astrocytes express functional CB_1 receptors in several brain regions [14,15,30,31], we investigated whether they might be accountable for the spatial spreading of eCB-induced inhibition in the spinal cord. To test this, we prepared spinal slices from mice expressing enhanced green fluorescent protein (EGFP) under the promoter of glial fibrillary acidic protein (GFAP) [32], and recorded visually identified astrocytes in the ventral horn using a patch-clamp electrode loaded with the Ca^{2+}-sensitive fluorophore Oregon Green. While blocking action potentials with tetrodotoxin (TTX) and synaptic transmission with cadmium chloride, we monitored variations in Ca^{2+} concentration by two-photon microscopy. We found that puff applications of the endocannabinoid 2-AG near the Oregon Green-loaded astrocyte induced large increases in intracellular Ca^{2+} (Fig. 4a-b), indicating that spinal ventral astrocytes express functional CB receptors as well as dorsal horn astrocytes [33]. We verified this by performing pharmacological tests while monitoring Ca^{2+} responses using epifluorescence microscopy. In the presence of TTX, the selective CB_1 antagonist AM281 abolished all responses to puff-applied 2-AG (Fig. 4c). Puff application of Ringer's at the same position failed to induce a response (n = 3; Fig. 4c). To determine whether these astrocytic CB_1 receptors are activated by depolarization-induced eCB release, we loaded slices with the cell-permeant Ca^{2+} indicator Rhod-2 AM and monitored Ca^{2+} concentration in astrocytes expressing EGFP. In the presence of TTX, we found that depolarization of a ventral horn interneuron was sufficient to trigger Ca^{2+} increases in neighboring astrocytes (Fig. 4d-f). Here again, the responses were abolished by AM281 (Fig. 4e-f), suggesting that eCBs released by neuronal depolarization induce activation of astrocytic CB_1 receptors, as reported previously in the hippocampus [14].

Next, we tested whether activation of astrocytes by eCBs is sufficient to inhibit excitatory synaptic transmission during DSE. While monitoring PPR in interneurons, we puff applied 2-AG close to a neighboring astrocyte (Fig. 5a) and found that it induced presynaptic inhibition (Fig. 5b,c,g,h). The degree of inhibition for synapses with high release probability (PPR<1; n=10) and low release probability (PPR>1; n=10) were similar (Mann Whitney test, p = 0.39). To verify that this inhibition was dependent on astrocytes, we buffered intracellular Ca^{2+} in the nearby astrocyte by loading it with the Ca^{2+} chelator BAPTA through a patch pipette (Fig. 5d). This eliminated the inhibitory effect of 2-AG on synaptic transmission (Fig. 5e-h), suggesting that DSE is mediated by astrocytes. To test this hypothesis, we monitored synaptic transmission in neurons expressing robust DSE (Fig. 5i-k,o,p). Loading a single neighboring astrocyte with BAPTA (Fig. 5l) was sufficient to abolish DSE (Fig. 5m-p). Together, these results demonstrate that DSE in the spinal cord is mediated by the action of eCBs on astrocytic CB receptors.

We previously showed that activation of ventral horn astrocytes causes them to release ATP, which is then converted to adenosine by extracellular ectonucleotidases. The subsequent activation of adenosine A1 receptors on presynaptic terminals inhibits excitatory neurotransmission, in a mechanism resembling that in the neocortex [34,35]. We hypothesized that this mechanism is responsible for the induction of presynaptic inhibition upon activation of astrocytic CB receptors. To test this hypothesis, we measured the effect of the selective ectonucleotidase inhibitor ARL 67156 on neurons that showed an increase in PPR in response to CB receptor activation by 2-AG (Fig. 6a-d,h). In the presence of ARL 67156, PPR remained unchanged upon CB receptor activation, indicating a lack of CB-induced

presynaptic inhibition (Fig. 6d-h). We also tested the effect of the selective adenosine A1 receptor antagonist DPCPX using a similar protocol. Here again, the compound abolished the increase in PPR and thus inhibition of synaptic transmission (Fig. 6i-p). To confirm the involvement of A1 receptors, we tested the effects of DPCX on DSE. As expected, A1 receptor block was sufficient to prevent depolarization-induced presynaptic inhibition (Fig. 6q-x). Our results demonstrate that DSE and presynaptic inhibition are caused by CB-induced release of purines from astrocytes acting on presynaptic A1 receptors.

Endocannabinoid-induced inhibition of synaptic transmission suppresses tremor *in vivo*

To verify that spinal astrocytic CB_1 receptors also induce DSE in adult mice, we used a conditional mutant mouse line in which tamoxifen administration induced knockout (KO) of CB_1 receptors in glial fibrillary acidic protein (GFAP)-positive cells (GFAP-CB_1-KO mice) [36]. Using immunohistochemical staining against CB_1 and GFAP, we confirmed that CB_1 receptor expression in the grey matter of the spinal cord was altered in tamoxifen-treated KO animals (GFAP-CB1-KO) compared to control littermates (GFAP-CB_1-WT). Specifically, the number of GFAP-positive astrocytes that co-expressed CB_1 was significantly reduced in GFAP-CB_1-KO mice (Supplementary Fig. 1). We tested whether DSE could be induced in these adult mice using spinal cord slices from adult animals and the same electrophysiological protocol used in juvenile slices. Postsynaptic depolarization of ventral spinal interneurons from control (GFAP-CB_1-WT) mice induced a reduction of evoked EPSCs (Fig. 7a-d) and a concomitant increase in PPR (Fig. 7h) in 7 out of 9 cells (78%). However, in slices from GFAP-CB_1-KO mice, DSE could not be evoked (13 cells, Fig. 7e-g). We also found that CB_1 KO unmasked inhibition of the second pulse in the paired protocol, resulting in the same decrease in PPR (Fig. 7h) that we observed following blockade of CB_1 receptors (Fig. 2). Taken together, these results confirm that DSE is mediated by spinal astrocytic CB_1 receptors in both juvenile and adult mice.

The experiments thus far demonstrate that activation of spinal astrocytic CB_1 receptors inhibits excitatory synaptic transmission and that intrathecal spinal injection of a CB receptor agonist suppresses tremor. If astrocytic CB_1 receptors are important for tremor reduction, knocking them out should abolish the anti-tremor effect of CB receptor agonists. We tested this hypothesis using our mutant mouse lines and found that both GFAP-CB_1-WT and GFAP-CB_1-KO adult mice responded to intraperitoneal administration of harmaline by exhibiting generalized tremor (Fig. 8), similar to that observed in wild-type animals (Fig. 1). This observation suggests that CB action on astrocytes is not involved in the propagation of rhythmic firing and generation of muscle tremor in this harmaline model. In contrast, intrathecal injection of the CB agonist WIN55,212-2 at the lumbar level suppressed tremor in GFAP-CB_1-WT mice (Fig. 8a-b) but had no noticeable effect in GFAP-CB_1-KO littermates (Fig. 8c-d). These results show that, upon CB_1 receptor activation, spinal astrocytes function as filters that suppress excessive neuronal rhythmicity by inhibiting excitatory transmission. Furthermore, they demonstrate that astrocytes must be considered as integral parts of neuronal networks involved in motor control.

Discussion

We investigated the harmaline model of essential tremor in juvenile and adult mice and found that depolarization of spinal interneurons releases eCBs that activate astrocytic CB_1 receptors, causing release of purines and subsequent inhibition of synaptic transmission between excitatory axons and these interneurons. We also showed that the anti-tremor action of WIN55,212-2 is dependent on these astrocytic CB_1 receptors. Our results clearly demonstrate that spinal astrocytes activated by eCBs are part of the network responsible for the generation of limb movements, and that purines permit communication between astrocytes and excitatory synapses on ventral horn interneurons. This agrees with previous data showing that neurons belonging to spinal neuronal networks responsible for motor control are modulated by purines released from astrocytes [35,37,38].

eCB receptors are expressed by astrocytes in other regions of the central nervous system, including the hippocampus, amygdala, and nucleus accumbens [17]. Activation of hippocampal astrocytes triggers glutamate release that can induce either facilitation of synaptic transmission by acting on presynaptic metabotropic receptors [15] or long-term depression by activating postsynaptic NMDA receptors [17]. In addition, hippocampal astrocytes can also promote long-term potentiation by releasing D-serine, which acts as a co-agonist on postsynaptic NMDA receptors [39]. Our data show that the activation of CB_1 receptors on spinal astrocytes releases purines that bind to presynaptic A1 receptors and inhibit excitatory synaptic transmission. Because eCBs are membrane-permeant lipid molecules that do not diffuse more than 20 μm away from their release site [40], their effect on presynaptic receptors is restricted to those that lie close to eCB release sites [12]. In contrast, eCB activation of astrocytes can affect the whole neuropil domain occupied by this cell type and therefore affect transmission at hundreds of synapses. In agreement with this, we found that heterosynaptic inhibition could spread more than 130 μm from the soma of the interneuron releasing eCBs. Thus, astrocytes are key elements for mediating the effects of eCB signaling in space.

Our data reveal that an essential function of astrocytic eCB signaling is to decrease pathological tremor. During motor activity, 10 Hz oscillations are carried from the motor cortex to the spinal cord, but these oscillations are not apparent in contracting muscles in normal physiological conditions [41]. In pathological situations, these tremors become visible, and the cerebellum or basal ganglia are important for their limitation. A spinal system local to the final motor output would have the advantage of providing a filter that can act on most forms of tremor. Our results show that spinal astrocytes are good candidates for providing such a filter.

Tremor is the most common movement disorder in humans, with a prevalence of 4% in people aged 40 and older. It can be idiopathic or triggered by injuries and neurodegenerative disease. Current therapies aim to decreasing the overall excitability of neurons by means of beta blockers such as propranolol or anticonvulsant medications like primidone [6]. These are often associated with adverse side effects, including fatigue, impotence, headache, bradycardia, depression, sedation, and nausea [6]. Our work, revealing a role for astrocytic eCB signaling in the reduction of tremor, opens up a potential route to develop novel therapies that target eCB receptors and/or astrocytes.

Methods

Animals

All experiments were conducted in strict compliance with the European Union recommendations (2010/63/EU) and were approved by the local ethical committee the Animal Experiments Inspectorate of Denmark (authorization number 2016-15-0201-01101 and 2018-15-0201-01463). In this study we have used wild type C57BL/6J mice purchased from Janvier Labs (France), transgenic mice expressing enhanced green fluorescent protein (E-GFP) under the promoter of glial fibrillary acidic protein [GFAP; line Tgn(hgFAPEGEP)] GFEC 335 (GFAP-GFP mice, kindly provided by Professor Frank Kirchhoff, University of Saarland, Homburg, Germany) as well as GFAP-CB1-KO mutant mice and their wild type littermates (GFAP-CB1-WT). The use of Transgenic mice GFAP-CB1-KO and GFAP-CB1-WT was approved by the local Committee on Animal Health and Care of Bordeaux and the French Ministry of Agriculture and Forestry (authorization number A33063098) and Committee of Ethics for Animal Welfare of the University of the Basque Country (CEEA/408/2015/Grandes Moreno, CEIAB/ 213/2015/Grandes Moreno). Animals were housed in groups under standard conditions in a day/night cycle of 12/12 h (light on at 7 am). Temperature: 22°C (+/- 2°C). Humidity: 55% +/- 10%. Behavioral experiments and *in vitro* electrophysiological experiments were conducted between 9 am and 6 pm.

GFAP-CB1-KO mice were generated using the CRE/loxP system [36]. Mice (CB1f/f) carrying the “floxed” CB1 encoding gene *CNR1* [42] were crossed with GFAP-CreERT2 mice [43], using a three-step backcrossing procedure to obtain CB1f/f;GFAP-CreERT2 and CB1f/f littermates, called GFAP-CB1-KO and GFAP-CB1-WT, respectively. Deletion of the CB1 encoding gene in young (3 weeks old, used for electrophysiological studies) or adult mice (8-10 weeks old, used for behavioral experiments and immunohistochemistry) was obtained by 8 days of daily i.p. injections of tamoxifen (Sigma-Aldrich, France; 0.5 mg for young mice and 1 mg for adults, dissolved at 10 mg/ml in 90% sesame oil, 10% ethanol). Mice were used 3-5 weeks after the last tamoxifen injection. Only female GFAP-CB1-WT and GFAP-CB1-KO were used.

Electrophysiology

Animals used: wild type (C57BL/6J; Janvier), GFAP-GFP, GFAP-CB1-KO and GFAP-CB1-WT After decapitation, the spinal cord of neonatal mice (P2-P15) was removed and submerged in Ringer’s Solution of the following composition (in mM): NaCl 125, KCl 2.5, $NaHCO_3$ 26, $CaCl_2$ 2, $MgCl_2$ 1, NaH_2PO_4 1.25, Glucose 25. Ringer’s solution was continuously carbogenated with 95% O_2 plus 5% CO_2. The lumbar enlargement was cut in slices (300 μm) by means of a vibratome (MicroM HM 650V; Microm International GmbH, Germany) equipped with a cooling unit set at 2°C. For experiments with adult animals (P50-P63), a cutting solution with the following composition was used (in mM): 130 K-gluconate, 15 KCl, 0.05 EGTA, 20 HEPES, 25 D-glucose, 3 kynurenic acid and adjusted to ph 7.4 with NaOH and the time from decapitation to first slice was <10 minutes. The slices were kept in oxygenated Ringer’s Solution in a recording chamber. Slices from adult animals were kept at 30° C. The pipette solution contained (in mM): 122 K-gluconate, 2.5 $MgCl_2$, 0.0003 $CaCl_2$, 2.8 Mg-gluconate, 5 K-HEPES, 5 H-HEPES, 5 Na_2ATP, 0.09 Alexa 488 hydrazide or

0.068 Alexa 568 hydrazide sodium salt (Life Technologies, USA), and KOH to adjust the pH to 7.4. Calcium-buffering pipette solution contained (in mM): 40 K- gluconate, 30 K_4-BAPTA, 2.5 $MgCl_2$, 0.0003 $CaCl_2$, 2.8 Mg-gluconate, 5 K-HEPES, 5 H-HEPES, 5 Na_2ATP, 0.068 Alexa 568 hydrazide sodium salt (Life Technologies, USA) and the necessary amount of KOH to adjust the pH to 7.4. Electrodes used had a resistance of 4 to 10 MΩ. Recordings where sampled at 10-20 kHz with a 16-bit analog-to-digital converter (DIGIDATA 1440; Molecular Devices, USA) and displayed by means of Clampex 10.2 software (Molecular Devices, USA).

Excitatory synaptic transmission was evoked by means of a bipolar stimulation electrode (TM33CCNON; World Precision Instruments, Sarasota, FL, USA) connected to an isolation unit (Isolator 11, Axon Instruments, USA) and positioned in the vicinity of the neuron recorded from. Ionotropic inhibitory transmission was blocked by gabazine (10 μM) and strychnine (1μM) added to the extracellular medium. Different locations were tried until an excitatory post synaptic current (EPSC) was evoked. Average EPSCs (8-10 sweeps) were used for quantification. Astrocytes expressing E-GFP in the GFEC 335 mouse line were visually identified by means of epifluorescence microscopy. DSE was induced by depolarizing voltage pulses (-70mV to 10mV for 0.5-2s). Test EPSCs were recorded 500 ms after the end of the depolarizing pulse. Recordings were discarded if the recorded cell became unstable. Data collection and analysis were not performed blind to the conditions of the experiments. Experimental procedures were not randomized.

Pharmacology

2-Arachidonylglycerol (10 μM in 0.01% DMSO, Tocris Bioscience, UK) was puff applied for 1s (14–35 Pa) by a homemade time-controlled pressure device. Puff pipettes were made from borosilicate capillaries (tip diameter ranging from 1.5–2 μm; BF150-86-7.5, Sutter Instrument, USA). The following compounds were applied to the bath: 1-(2,4-Dichlorophenyl)-5-(4-iodophenyl)-4-methyl-*N*-4-morpholinyl-1*H*-pyrazole-3-carboxamide (AM281; 1μM for *in vitro* experiments and 0.5mg/kg for *in vivo* experiments; Sigma–Aldrich, USA), $CdCl_2$, (100μM, Sigma–Aldrich, St. Louis, MO, USA), Tetrodotoxin (1 μM; Alomone Labs, Israel), 8-Cyclopentyl-1,3-dipropylxanthine (DPCPX, 5 μM in 0.1% DMSO; Tocris Bioscience, UK), 6-N,N-Diethyl-D-β,γ-dibromomethylene ATP trisodium salt (ARL 67156 trisodium salt, 50 μM; Tocris Bioscience, UK).

Calcium imaging

Calcium imaging in astrocytes was performed after patching visually identified astrocytes expressing EGFP (see above). The patch solution contained the cell impermeant calcium indicator Oregon Green™ 488 BAPTA-1, Hexapotassium Salt, (OGB; 100 μM, Invitrogen, USA). The slice was then transferred under the objective of a multiphoton microscope (Bergamo II Series, Thorlabs Inc., Newton, New Jersey, USA) equipped with a Ti:sapphire laser Chameleon Ultra II Laser (Coherent, Santa Clara, CA, USA) and controlled by ThorImageLS software 3.0. The Laser was tuned at 950 nm. Fluorescence was split into red and green channels with a dichroic reflector (562nm single-edge) and detected via a 500/550 nm bandpass filters (Semrock, USA) using photomultiplier tubes (Ultrasensitive GaAsP PMTs Positioned Directly Behind the Objective). For experiments using pharmacology,

imaging was performed under the objective of a epifluorescence microscope (BX51WI, Olympus, Japan) with the use of LED illumination (X-Cite® 120LEDBoost, Canada). Recordings were obtained with a Zyla sCMOS Camera (Andor, UK). Pictures were acquired at 8-30 frames/second. Images were analyzed with ImageJ software (National Institutes of Health, USA). Regions of interest (ROIs) were defined offline and quantified with ImageJ (Fiji, www.fiji.sc). Potential bleaching was corrected by subtracting the linear regression of the signal. The relative change of fluorescence signal ΔF/F was calculated as $(F_1-F_0)/F_0$., where F_1 represents the intensity of the signal at a given time and F_0 the baseline of the signal. A response was considered significant when it exceeded twice the standard deviation of the baseline signal for at least 3 consecutive points. Data collection and analysis were not performed blind to the conditions of the experiments. Experimental procedures were not randomized.

Measurement of tremor

Animals used: 8-14 weeks old wild type (C57BL/6J; Janvier), GFAP-CB1-KO and GFAP-CB1-WT. The mice were placed in a custom-made cage (15cm x 15cm x 20cm) suspended from a metal rack by rubber bands (for details, see [22]). Underneath the cage was attached an iPhone 7 (Apple, USA). Tremor measurements were obtained with the VibSensor app (v.2.0.0., Now Instruments and Software, Inc., USA). The VibSensor app measures acceleration in three perpendicular axes by using the inbuilt accelerometer of the phone. Tremor data were sampled in 10 minutes episodes at 100Hz. Data collection and analysis were not performed blind to the conditions of the experiments. Experimental procedures were randomized by simple randomization according to treatment type and genotype.

Harmaline induced tremor and intrathecal injection

Tremor was induced by intraperitoneal injection of harmaline hydrochloride (30mg/kg; Sigma–Aldrich, USA). For some control experiments, AM281 (0.5mg/kg) was injected intraperitoneal simultaneous. Tremor appeared within 10 minutes and a 10-minute baseline recording was performed. If harmaline failed to induce a consistent tremor, the experiments were discontinued. 20 minutes after harmaline injection, animals where anaesthetized with isoflurane (4%, 400 ml oxygen flow/min) in an induction chamber. Anesthesia was maintained with a nosecone (1.5%, 400 ml oxygen flow/min), while an intrathecal injection (10μl WIN55,212-2 30mg/ml or saline) was performed using a 27G needle. The injection was delivered intrathecal to the lumbar level (L3-S1), and correct needle placement was determined by leg or tail flick. Mice without clear flick response were excluded from the study. Intrathecal injections were performed by a blinded researcher. Animals were placed back in the custom-made cage and left to recover for 30 minutes before a new 10 min tremor recording was made.

Immunohistochemistry

Animals were sacrificed and lumbar parts of spinal cords were post fixed in 4% paraformaldehyde (PFA) in phosphate buffered saline (PBS, 0.1M, pH 7.4). Serial 10-μm-thick coronal sections from GFAP-CB1-WT and GFAP-CB1-KO mice obtained with cryostat were processed in parallel. Free-floating sections were rinsed in PBS, permeabilized with 10% normal donkey serum in PBS with 0.3% Triton X-100 (PBS-Tx) for 1 h at room

temperature (RT) and incubated with goat polyclonal anti-CB1 antibody (1:1000, #CB1-GO-Af450, Frontier Institute) for 7 hours at RT. Afterwards, rabbit polyclonal anti-GFAP (1:500, #ZO334, Dako) antibody was added and the sections were further incubated with both antibodies overnight at 4°C (total time of incubation for anti-CB1 was 24 h). The next day, sections were washed in PBS and incubated for 2 hours at RT with secondary antibodies: Alexa fluor donkey anti-goat 555 (1:500, Life Technologies) and Alexa fluor donkey anti-rabbit 488 (1:500, Life Technologies) and then washed in PBS. Finally, sections were incubated with DAPI (1:20 000, Fisher Scientific) for 5 minutes before being washed, mounted using Fluoromount-G (#17984-25, Electron Microscopy Sciences) and cover slipped. Validation of abovementioned antibodies is available in the Nature Research Reporting Summary linked to this article. The fluorescence was visualized with an epifluorescence Leica DM6000 microscope. The contrast and brightness were altered for illustration purposes.

Numerical evaluation for immunohistochemistry

Semi-quantification of CB1 and GFAP signals was performed using ImageJ version 1.52a. For automated detection of CB1 particles from the background, binary images were generated using Threshold function that was the same for all analyzed pictures. Co-expression of CB1 particles with GFAP+ cells was counted manually in grey matter of individual spinal cord sections of GFAP-CB1-WT (n=3 mice, 9 sections, 539 astrocytes, 528 CB1 signals) and GFAP-CB1-KO (n=3 mice, 9 sections, 602 astrocytes, 537 CB1 signals) mice using Synchronize Windows and Cell Counter plugins. Data collection and analysis were not performed blind to the conditions of the experiments. Experimental procedures were not randomized.

Analysis

Data are represented as mean ± standard deviation of the mean. Data analysis of electrophysiological recordings were performed in Clampfit 10.5.1.0 software (Molecular Devices, USA) and Graphpad Prism 8 (GraphPad Software, USA). Flourescence images and tremor measurements were analyzed with Graphpad Prism 8 (GraphPad Software, USA), Python programming language 3.8.5. (Python Software Foundation, https://www.python.org/) and JupiterLab version 2.1.5 (https://jupyter.org).

Statistics

Statistical significance was assessed by Student’s t test, Mann-Whitney test and Wilcoxon matched-pairs signed rank test. Due to the small sample size, data obtained from elecrophysiological and behavioral experiments were not assumed to be normally distributed and non-parametric tests were used. For immunohistochemistry data distribution was assessed using D’Agostino & Pearson normality test. Significance levels are: * P<0.05, ** P<0.01, *** P<0.001.

Supplementary Material

Refer to Web version on PubMed Central for supplementary material.

Acknowledgements

We thank Professor Frank Kirchhoff (University of Saarland) for providing the Tgn(hgFAPEGEP) mice, Dr Marco Beato (UCL) for his help with the adult spinal cord slice preparation, Dr Alex Fletcher-Jones and Dr Abel Eraso for technical support and Lesley Anson for her help in editing the manuscript. The study was funded by Offerfonden (JFP), Aase og Ejnar Danielsens Fond (EMC), Den Owensenske Fond (JFP), Læge Sofus Carl Emil Friis og hustru Olga Doris Fond (JFP), Danmarks Frie Forskningsfond (9039-00072B to JFP), European Research Council (grant MiCaBra, ERC-2017-AdG-786467 to GM) and Fondation pour la Recherche Médicale (grant no. FRM SPF201809006908 to US).

Data Availability

Electrophysiological, imaging and tremor data are available at zenodo.org: DOI: 10.5281/zenodo.4478494. Data for immunohistochemistry are available from the corresponding author upon reasonable request.

Code availability

Codes written for data analysis of this study is available at https://github.com/perrierlab/Carlsen_et_al_2021

References

1. Deuschl G, Bain P, Brin M. Consensus statement of the Movement Disorder Society on Tremor. Ad Hoc Scientific Committee. Movement disorders : official journal of the Movement Disorder Society. 1998; 13(Suppl 3):2–23. DOI: 10.1002/mds.870131303
2. Alty JE, Kempster PA. A practical guide to the differential diagnosis of tremor. Postgrad Med J. 2011; 87:623–629. DOI: 10.1136/pgmj.2009.089623 [PubMed: 21690256]
3. Biary N, Cleeves L, Findley L, Koller W. Post-traumatic tremor. Neurology. 1989; 39:103–106. DOI: 10.1212/wnl.39.1.103 [PubMed: 2909897]
4. Koch M, Mostert J, Heersema D, De Keyser J. Tremor in multiple sclerosis. J Neurol. 2007; 254:133–145. DOI: 10.1007/s00415-006-0296-7 [PubMed: 17318714]
5. Rinker JR 2nd, et al. Prevalence and characteristics of tremor in the NARCOMS multiple sclerosis registry: a cross-sectional survey. BMJ Open. 2015; 5:e006714. doi: 10.1136/bmjopen-2014-006714
6. Louis ED. Essential tremors: a family of neurodegenerative disorders? Arch Neurol. 2009; 66:1202–1208. DOI: 10.1001/archneurol.2009.217 [PubMed: 19822775]
7. Consroe P, Musty R, Rein J, Tillery W, Pertwee R. The perceived effects of smoked cannabis on patients with multiple sclerosis. Eur Neurol. 1997; 38:44–48. DOI: 10.1159/000112901
8. Clifford DB. Tetrahydrocannabinol for tremor in multiple sclerosis. Ann Neurol. 1983; 13:669–671. DOI: 10.1002/ana.410130616 [PubMed: 6309074]
9. Meinck HM, Schonle PW, Conrad B. Effect of cannabinoids on spasticity and ataxia in multiple sclerosis. J Neurol. 1989; 236:120–122. [PubMed: 2709054]
10. Arjmand S, et al. Cannabinoids and Tremor Induced by Motor-related Disorders: Friend or Foe? Neurotherapeutics. 2015; 12:778–787. DOI: 10.1007/s13311-015-0367-5 [PubMed: 26152606]
11. Baker D, et al. Cannabinoids control spasticity and tremor in a multiple sclerosis model. Nature. 2000; 404:84–87. DOI: 10.1038/35003583 [PubMed: 10716447]
12. Wilson RI, Nicoll RA. Endogenous cannabinoids mediate retrograde signalling at hippocampal synapses. Nature. 2001; 410:588–592. DOI: 10.1038/35069076 [PubMed: 11279497]
13. Kreitzer AC, Regehr WG. Retrograde inhibition of presynaptic calcium influx by endogenous cannabinoids at excitatory synapses onto Purkinje cells. Neuron. 2001; 29:717–727. [PubMed: 11301030]
14. Navarrete M, Araque A. Endocannabinoids mediate neuron-astrocyte communication. Neuron. 2008; 57:883–893. DOI: 10.1016/j.neuron.2008.01.029 [PubMed: 18367089]

15. Navarrete M, Araque A. Endocannabinoids Potentiate Synaptic Transmission through Stimulation of Astrocytes. Neuron. 2010; 68:113–126. doi: 10.1016/j.neuron.2010.08.043 [PubMed: 20920795]
16. Navarrete M, Diez A, Araque A. Astrocytes in endocannabinoid signalling. Philos Trans R Soc Lond B Biol Sci. 2014; 369:20130599. doi: 10.1098/rstb.2013.0599 [PubMed: 25225093]
17. Metna-Laurent M, Marsicano G. Rising stars: modulation of brain functions by astroglial type-1 cannabinoid receptors. Glia. 2015; 63:353–364. DOI: 10.1002/glia.22773 [PubMed: 25452006]
18. Rodriguez JJ, Mackie K, Pickel VM. Ultrastructural localization of the CB1 cannabinoid receptor in mu-opioid receptor patches of the rat Caudate putamen nucleus. J Neurosci. 2001; 21:823–833. [PubMed: 11157068]
19. Piomelli D, Beltramo M, Giuffrida A, Stella N. Endogenous cannabinoid signaling. Neurobiol Dis. 1998; 5:462–473. DOI: 10.1006/nbdi.1998.0221 [PubMed: 9974178]
20. Kjaerulff O, Kiehn O. Distribution of networks generating and coordinating locomotor activity in the neonatal rat spinal cord in vitro: a lesion study. J Neurosci. 1996; 16:5777–5794. [PubMed: 8795632]
21. Llinas R, Volkind RA. The olivo-cerebellar system: functional properties as revealed by harmaline-induced tremor. Exp Brain Res. 1973; 18:69–87. [PubMed: 4746753]
22. Carlsen EMM, Amrutkar DV, Nielsen KS, Perrier JF. Accurate and affordable assessment of physiological and pathological tremor in rodents with the accelerometer of a smartphone. J Neurophysiol. 2019; doi: 10.1152/jn.00281.2019
23. Handforth A. Harmaline tremor: underlying mechanisms in a potential animal model of essential tremor. Tremor Other Hyperkinet Mov (N Y). 2012; 2 doi: 10.7916/D8TD9W2P
24. Sykova E, Nicholson C. Diffusion in brain extracellular space. Physiol Rev. 2008; 88:1277–1340. DOI: 10.1152/physrev.00027.2007 [PubMed: 18923183]
25. Wolf DA, et al. Dynamic dual-isotope molecular imaging elucidates principles for optimizing intrathecal drug delivery. JCI Insight. 2016; 1:e85311. doi: 10.1172/jci.insight.85311 [PubMed: 27699254]
26. McAuley JH, Marsden CD. Physiological and pathological tremors and rhythmic central motor control. Brain. 2000; 123(Pt 8):1545–1567. DOI: 10.1093/brain/123.8.1545 [PubMed: 10908186]
27. Chevaleyre V, Takahashi KA, Castillo PE. Endocannabinoid-mediated synaptic plasticity in the CNS. Annu Rev Neurosci. 2006; 29:37–76. DOI: 10.1146/annurev.neuro.29.051605.112834 [PubMed: 16776579]
28. Araque A, Castillo PE, Manzoni OJ, Tonini R. Synaptic functions of endocannabinoid signaling in health and disease. Neuropharmacology. 2017; 124:13–24. DOI: 10.1016/j.neuropharm.2017.06.017 [PubMed: 28625718]
29. Zucker RS, Regehr WG. Short-term synaptic plasticity. Annu Rev Physiol. 2002; 64:355–405. DOI: 10.1146/annurev.physiol.64.092501.114547 [PubMed: 11826273]
30. Oliveira da Cruz JF, Robin LM, Drago F, Marsicano G, Metna-Laurent M. Astroglial type-1 cannabinoid receptor (CB1): A new player in the tripartite synapse. Neuroscience. 2016; 323:35–42. DOI: 10.1016/j.neuroscience.2015.05.002 [PubMed: 25967266]
31. Gomez-Gonzalo M, et al. Endocannabinoids Induce Lateral Long-Term Potentiation of Transmitter Release by Stimulation of Gliotransmission. Cereb Cortex. 2015; 25:3699–3712. DOI: 10.1093/cercor/bhu231 [PubMed: 25260706]
32. Nolte C, et al. GFAP promoter-controlled EGFP-expressing transgenic mice: a tool to visualize astrocytes and astrogliosis in living brain tissue. Glia. 2001; 33:72–86. DOI: 10.1002/1098-1136(20010101)33:1<72::AID-GLIA1007>3.0.CO;2-A [PubMed: 11169793]
33. Hegyi Z, et al. CB1 receptor activation induces intracellular Ca(2+) mobilization and 2-arachidonoylglycerol release in rodent spinal cord astrocytes. Scientific reports. 2018; 8:10562. doi: 10.1038/s41598-018-28763-6 [PubMed: 30002493]
34. Lalo U, et al. Exocytosis of ATP from astrocytes modulates phasic and tonic inhibition in the neocortex. PLoS Biol. 2014; 12:e1001747. doi: 10.1371/journal.pbio.1001747 [PubMed: 24409095]

35. Carlsen EM, Perrier JF. Purines released from astrocytes inhibit excitatory synaptic transmission in the ventral horn of the spinal cord. Frontiers in neural circuits. 2014; 8:60. doi: 10.3389/fncir.2014.00060 [PubMed: 24926236]

36. Han J, et al. Acute cannabinoids impair working memory through astroglial CB1 receptor modulation of hippocampal LTD. Cell. 2012; 148:1039–1050. DOI: 10.1016/j.cell.2012.01.037 [PubMed: 22385967]

37. Broadhead MJ, Miles GB. Bi-Directional Communication Between Neurons and Astrocytes Modulates Spinal Motor Circuits. Front Cell Neurosci. 2020; 14:30. doi: 10.3389/fncel.2020.00030 [PubMed: 32180706]

38. Witts EC, Panetta KM, Miles GB. Glial-derived adenosine modulates spinal motor networks in mice. J Neurophysiol. 2012; 107:1925–1934. doi: 10.1152/jn.00513.2011 [PubMed: 22205649]

39. Robin LM, et al. Astroglial CB1 Receptors Determine Synaptic D-Serine Availability to Enable Recognition Memory. Neuron. 2018; 98:935–944 e935. DOI: 10.1016/j.neuron.2018.04.034 [PubMed: 29779943]

40. Alger BE. Retrograde signaling in the regulation of synaptic transmission: focus on endocannabinoids. Prog Neurobiol. 2002; 68:247–286. [PubMed: 12498988]

41. Williams ER, Baker SN. Renshaw cell recurrent inhibition improves physiological tremor by reducing corticomuscular coupling at 10 Hz. J Neurosci. 2009; 29:6616–6624. DOI: 10.1523/JNEUROSCI.0272-09.2009 [PubMed: 19458232]

Methods only references

42. Marsicano G, et al. CB1 cannabinoid receptors and on-demand defense against excitotoxicity. Science. 2003; 302:84–88. DOI: 10.1126/science.1088208 [PubMed: 14526074]

43. Hirrlinger PG, Scheller A, Braun C, Hirrlinger J, Kirchhoff F. Temporal control of gene recombination in astrocytes by transgenic expression of the tamoxifen-inducible DNA recombinase variant CreERT2. Glia. 2006; 54:11–20. DOI: 10.1002/glia.20342 [PubMed: 16575885]

Europe PMC Funders Author Manuscripts

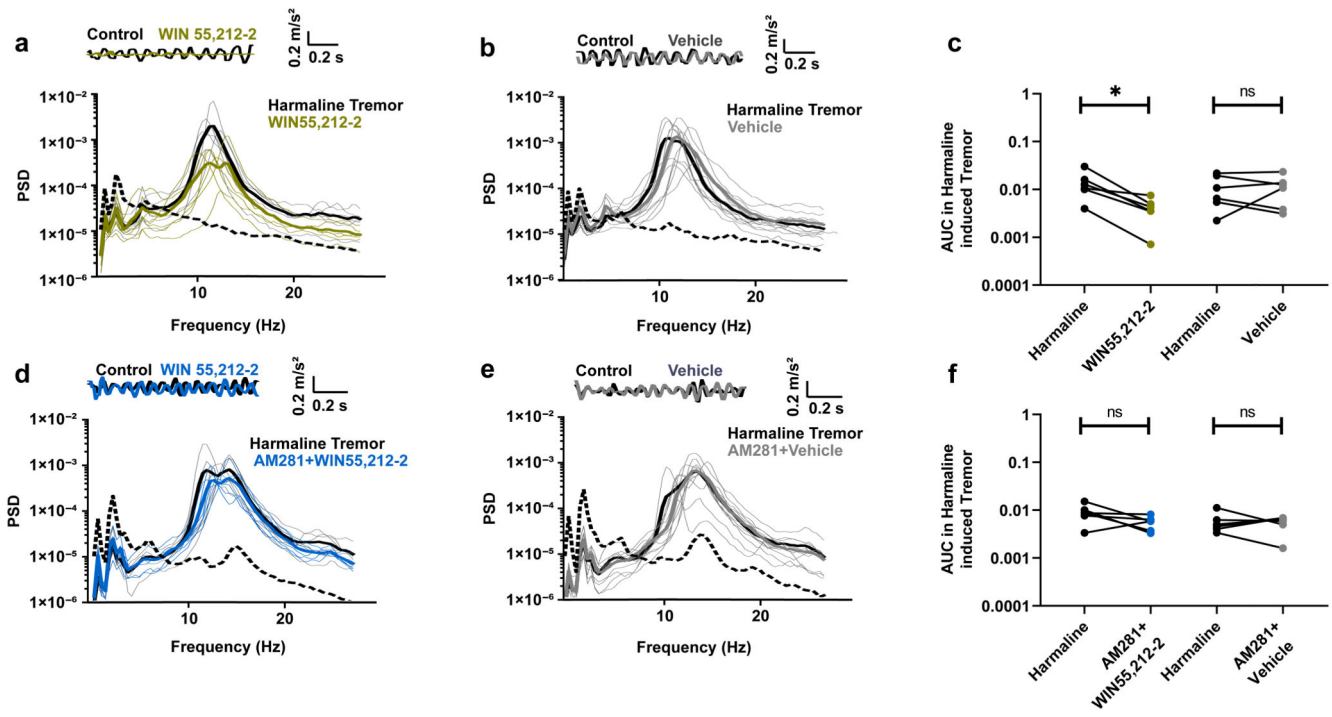

Fig. 1. Activation of CB receptors in the spinal cord has an anti-tremor effect.

a,b,d,e, Top: accelerometer traces. Bottom: power spectra of whole animal tremor. Dotted lines: examples of spontaneous tremor occurring before harmaline treatment. **a**, Administration of harmaline induced a tremor that was inhibited by intrathecal injection of WIN55,212-2. **b**, Intrathecal injection of a vehicle had no effect on harmaline-induced tremor. **c**, Area under the power spectra curve (8Hz-25Hz). Each dot pair corresponds to one animal. Significant effect of WIN55,212-2 (Wilcoxon matched-pairs signed rank test, n = 6, p = 0.031). No significant effect of vehicle (Wilcoxon matched-pairs signed rank test, n = 6, p = 0.99). **d**, When animals were pretreated with CB1 receptor antagonist AM281 (0.5mg/kg), WIN55,212-2 did not decrease tremor significantly. **e**, Pretreatment with AM281 and subsequent intrathecal injection of a vehicle had no effect on tremor. **f**, Area under the power spectra curve (8Hz-25Hz). Each dot pair corresponds to one animal. For animals pretreated with AM281, no significant effect of WIN55,212-2 (Wilcoxon matched-pairs signed rank test, n = 6, p = 0.16) or of vehicle (Wilcoxon matched-pairs signed rank test, n = 6, p = 0.99). The statistical test used was two-sided.

Europe PMC Funders Author Manuscripts

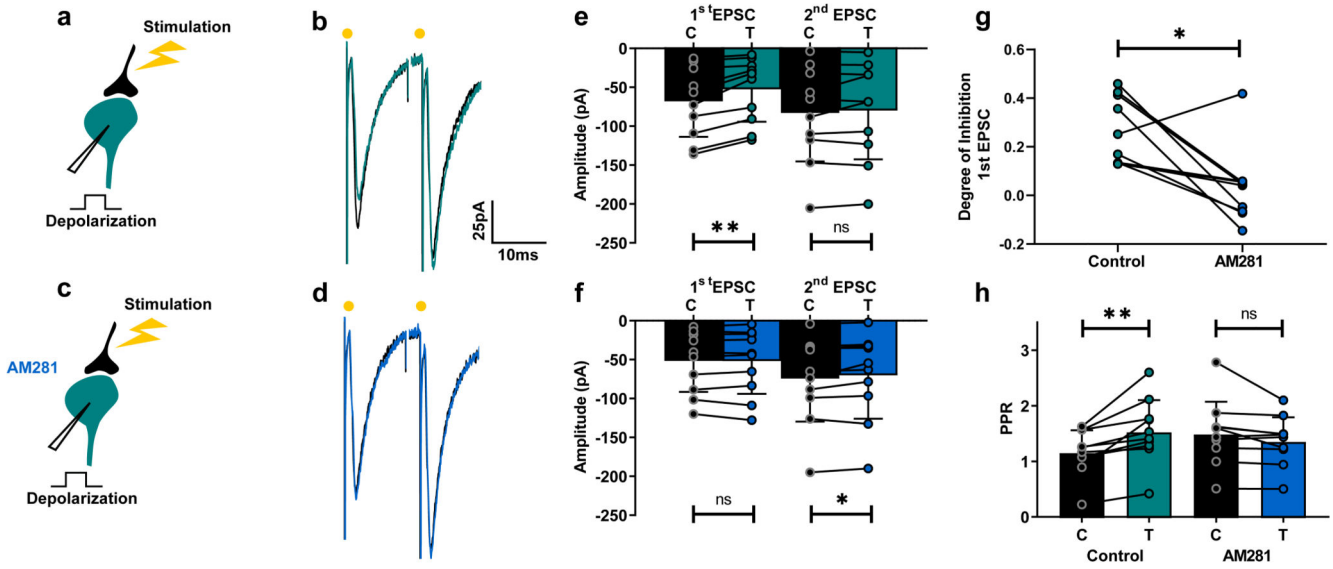

Fig. 2. Depolarization of ventral horn interneurons induces suppression of excitatory synaptic transmission

a,c, Schematic of spinal cord slice recordings. **b**, Example average response (10 sweeps) of an interneuron to electric stimulation of excitatory afferents before (black) and after a depolarizing pulse (turquoise). **d**, Same protocol in presence of AM281 (blue). **e**, Mean EPSC amplitudes from all cells tested before and after depolarization. First EPSC: significant inhibition (Wilcoxon matched-pairs signed rank test, n = 10 individual cells, p = 0.002); second EPSC: non-significant difference Wilcoxon matched-pairs signed rank test, n = 10 individual cells, p = 0.85). **f**, AM281 prevent induction of DSE (first EPSC: Wilcoxon matched-pairs signed rank test, n = 10 individual cells, p = 0.92; second EPSC: Wilcoxon matched-pairs signed rank test, n = 10 individual cells, p = 0.049). **g**, Degree of inhibition of first EPSC in control conditions and in the presence of AM281 (Wilcoxon matched-pairs signed rank test, n = 10 individual cells, p = 0.014). **h**, PPR before and after depolarization in control conditions and following addition of AM281. Significant increase in control (Wilcoxon matched-pairs signed rank test, n = 10 individual cells, p = 0.002). No significant change in AM281 (Wilcoxon matched-pairs signed rank test, n = 10 individual cells, p = 0.065). Data are presented as mean values +/- SD. The statistical test used was two-sided.

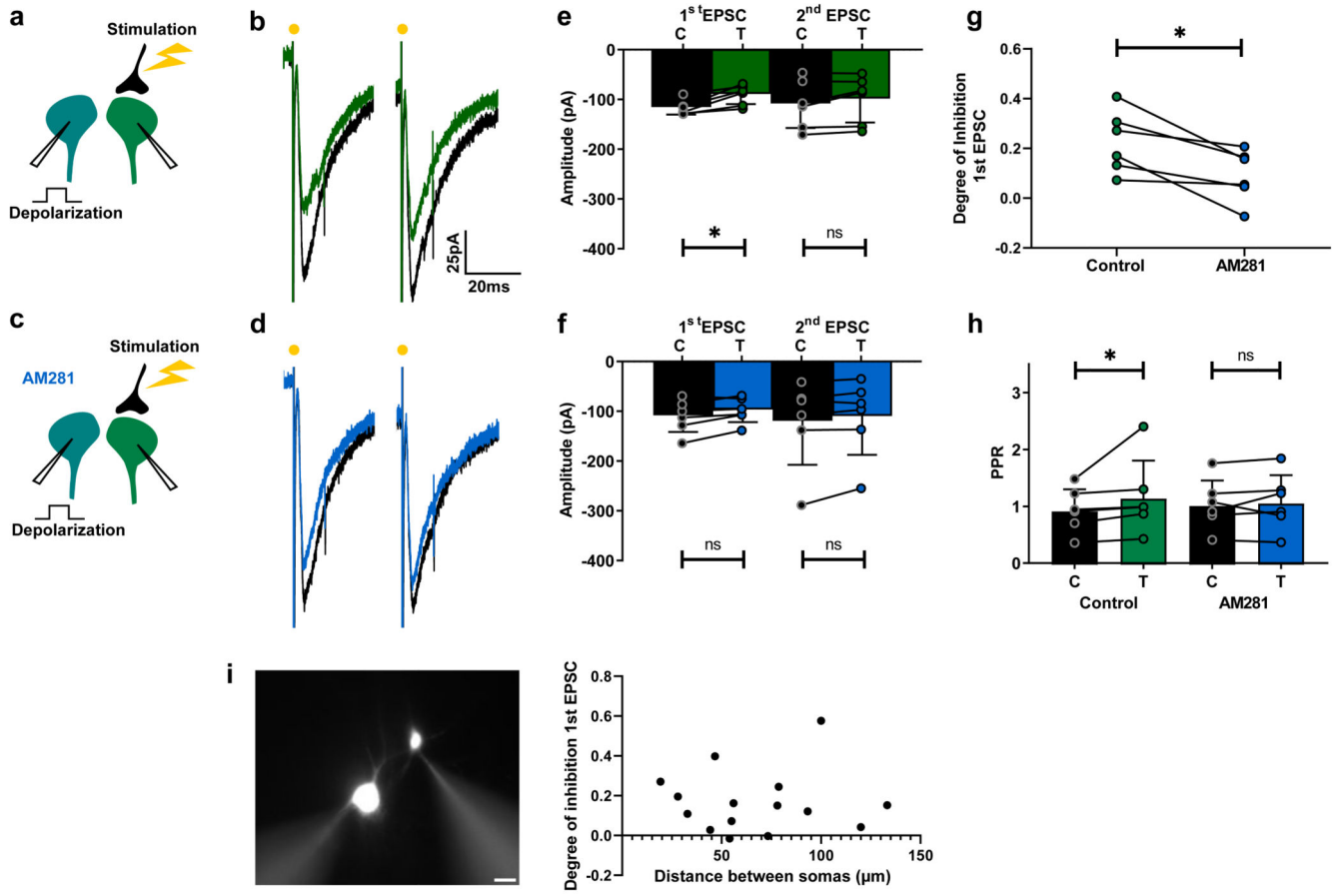

Fig. 3. DSE in the spinal cord occurs between interneurons

a,**c**, Schematic of spinal cord slice recordings. **b**, Example average response (10 sweeps) of an interneuron to electric stimulation before (black) and after depolarization of another interneuron (green). **d**, Same protocol in presence of AM281 (blue). **e**, mean EPSC amplitudes from all cells tested before and after depolarization. First EPSC: significant inhibition (Wilcoxon matched-pairs signed rank test, n = 6 individual cells, p = 0.031); second EPSC, no significant difference (Wilcoxon matched-pairs signed rank test, n = 6 individual cells, p = 0.16). **f**, Mean EPSC amplitudes before and after depolarization in the presence of AM281. No significant change induced by depolarization. (Wilcoxon matched-pairs signed rank test, n =6 individual cells: first EPSC, p = 0.09; second EPSC, p = 0.09). **g**, Degree of depolarization-induced inhibition of first EPSC in control conditions and after AM281. Significant difference (Wilcoxon matched-pairs signed rank test, n = 6 individual cells, p = 0.031). **h**, PPR before and after depolarization in control conditions and following addition of AM281. Significant increase in control (Wilcoxon matched-pairs signed rank test, n = 6 individual cells, p = 0.031). No significant change in AM281 (Wilcoxon matched-pairs signed rank test, n = 6 individual cells, p = 0.43). **i**, Epifluorescence image of an example pair of neurons recorded in whole-cell configuration. Scalebar: 20 µm. Plot: degree of inhibition as function of distance between somas for all pairs measured (n=15 pairs). Data are presented as mean values +/- SD. The statistical test used was two-sided.

Europe PMC Funders Author Manuscripts

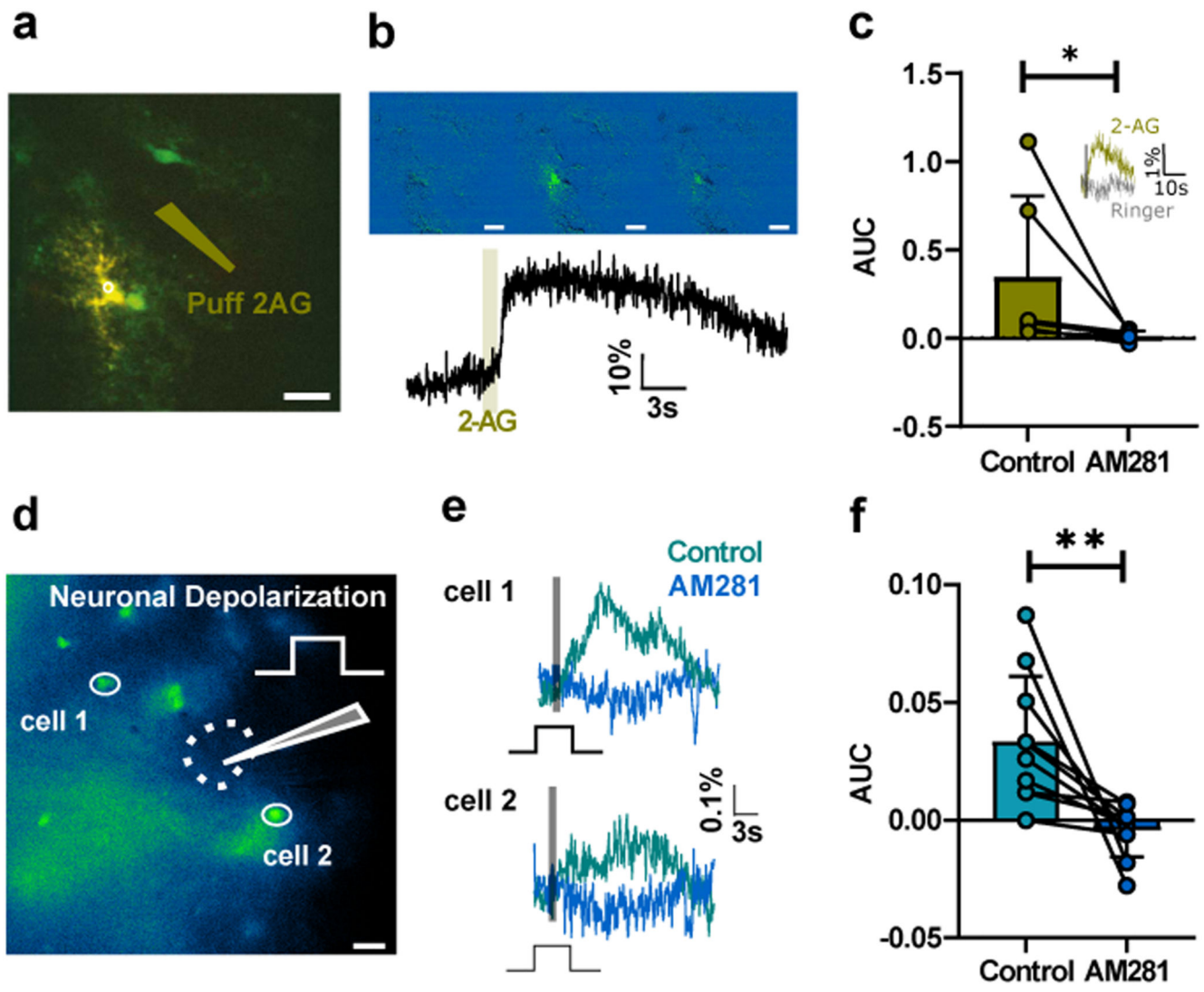

Fig. 4. Neuronal depolarization activates astrocytic CB_1 receptors

a, Single GFP-expressing astrocyte loaded with Oregon Green TTX (1 μM) and cadmium chloride (100 μM) present in the bath. Puff pipette loaded with 2-AG (10 μM) (olive). **b**, Cell activity monitored by two-photon microscopy before and after puff application of 2-AG (average response, 15±7%, n = 6 individual cells). **c**, Area under the curve (AUC) of the Ca^{2+} response monitored with epifluorescence microscopy following puff application of 2-AG in the presence of TTX (1μm), before and after addition of AM281. Significant reduction (Wilcoxon matched-pairs signed rank test, p = 0.031, n = 6 individual cells). Insert: A puff or Ringer's (same position, same intensity) had no effect (n = 3 individual cells). **d.** Example slice: GFP expression in a Rhod-2-AM loaded slice from the GFAP-GFP mouse. Whole-cell recording of an interneuron (position indicated by the dotted line) while monitoring Ca^{2+} in two GFP-positive cells stained with Rhod-2 by means of epifluorescence microscopy. Recording performed in TTX (1 μM). Scalebar: 20 μm. **e**, One-second depolarization of the interneuron (grey bar) induced an increase in Ca^{2+} for both cells depicted in d (mean of 3 consecutive trials). The responses were abolished by AM281

(1μM). **f**, AUC before and after AM281 for all tested cells. Significant decrease (Wilcoxon matched-pairs signed rank test, n = 10 cells from 3 animals, p = 0.002). Data are presented as mean values +/- SD. The statistical test used was two-sided.

Europe PMC Funders Author Manuscripts

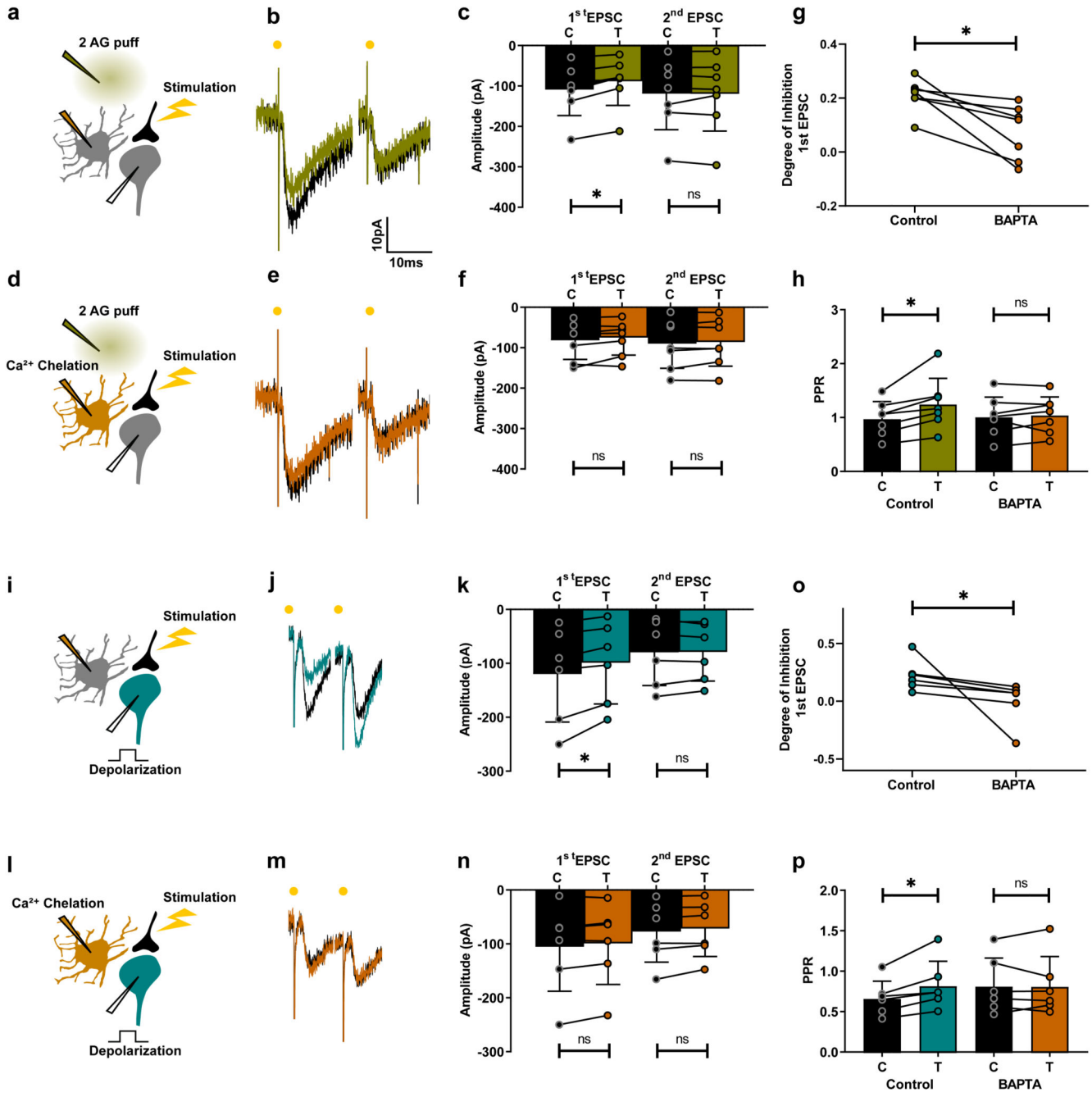

Fig. 5. DSE in the ventral horn is mediated by astrocytes

a, **d**, **i**, **l**, Schematic of spinal cord slice recordings. Patch pipette containing BAPTA (30 mM) (orange) cell-attached to an astrocyte. Puff pipette filled with 2-AG (10 μM). **b**, Example average response (10 sweeps) of an interneuron to electric stimulation of excitatory axons before (black) and after 2-AG puff (olive). **c**, Mean amplitude EPSCs from all cells tested before and after puff. First EPSC: significant inhibition (Wilcoxon matched-pairs signed rank test, n = 7 individual cells, p = 0.016); second EPSC, no significant difference (Wilcoxon matched-pairs signed rank test, n = 7 individual cells, p = 0.58). **d-f**, Same

Europe PMC Funders Author Manuscripts

protocol after breaking into the astrocytes (orange). No significant change induced by 2-AG (Wilcoxon matched-pairs signed rank test, n = 7 individual cells; first EPSC, p = 0.22; second EPSC, p = 0.58). **g**, Degree of inhibition of first EPSC. Significant difference (Wilcoxon matched-pairs signed rank test, n = 7 individual cells, p = 0.016). **h**, PPR before and after 2-AG in control conditions and after BAPTA loading of astrocyte. Significant increase in control (Wilcoxon matched-pairs signed rank test, n = 7 individual cells, p = 0.016). No significant change after BAPTA (Wilcoxon matched-pairs signed rank test, n = 7 individual cells, p = 0.58). **i-p**, Same protocol except that inhibition is induced by postsynaptic depolarization (turquoise). **k**, First EPSC: significant inhibition (Wilcoxon matched-pairs signed rank test, n = 6 individual cells, p = 0.031); second EPSC, no significant difference (Wilcoxon matched-pairs signed rank test, n = 6 individual cells, p = 0.84). **n**, After BAPTA, first EPSC (Wilcoxon matched-pairs signed rank test, n = 6 individual cells, p = 0.16); second EPSC (Wilcoxon matched-pairs signed rank test, n = 6 individual cells, p = 0.06). **o**, Significant inhibition (Wilcoxon matched-pairs signed rank test, n = 6 individual cells, p = 0.031). **p**, PPR before and after depolarization in control conditions and after BAPTA. Significant increase in control (Wilcoxon matched-pairs signed rank test, n = 6 individual cells, p = 0.031). No significant change after BAPTA (Wilcoxon matched-pairs signed rank test, n = 6 individual cells, p = 0.99). Data are presented as mean values +/- SD. The statistical test used was two-sided.

Europe PMC Funders Author Manuscripts

Europe PMC Funders Author Manuscripts

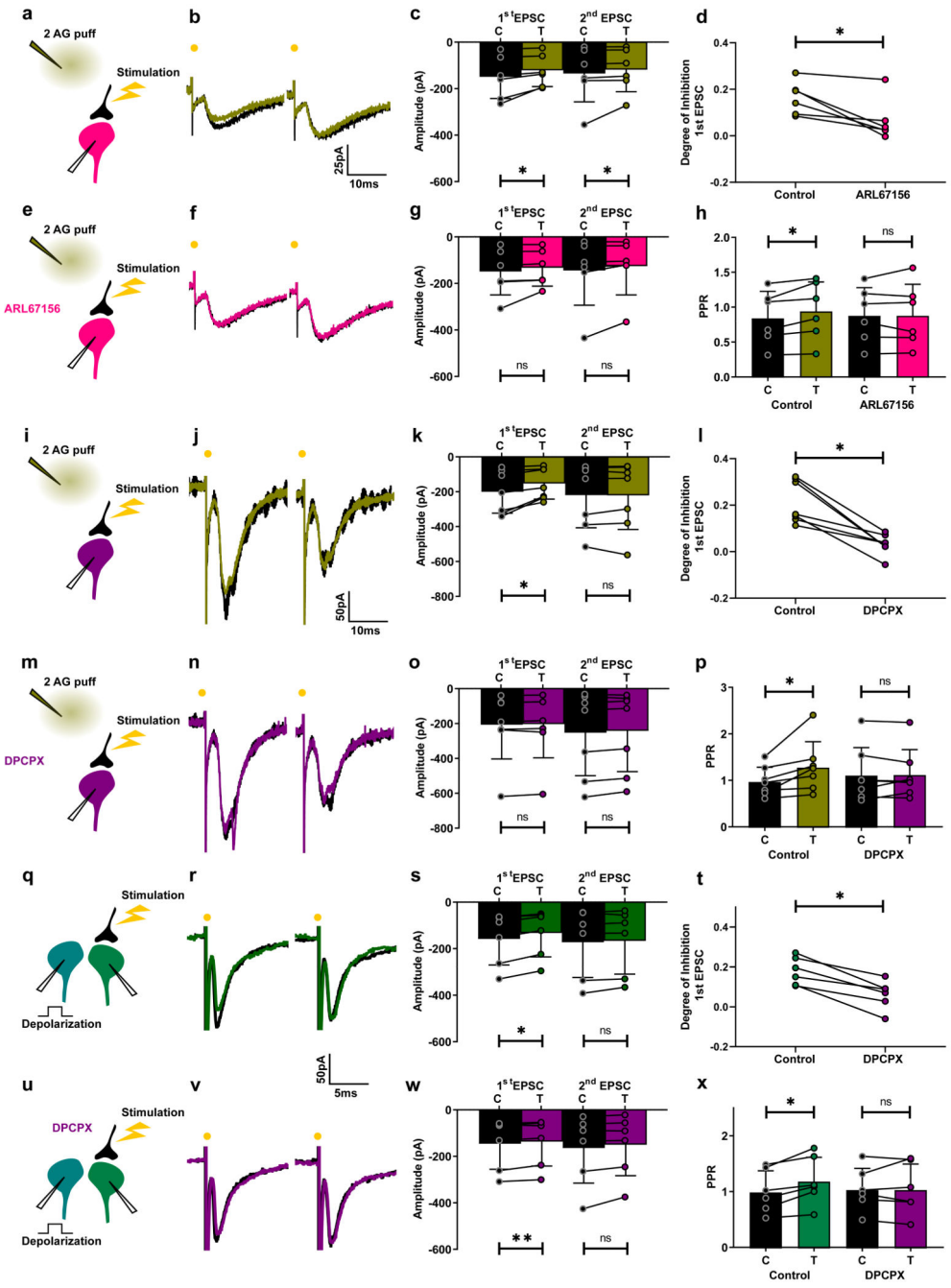

Fig. 6. Purines mediate suppression of excitation induced by 2-AG and depolarization.

a, **e**, **i**, **m**, **q**, **u**, Schematic of spinal cord slice recordings. Puff pipette filled with 2-AG (10 μM). **b**, Example average response (10 sweeps) of an interneuron to electric stimulation of excitatory axons before (black) and after 2-AG puff (olive). **c**, Mean amplitude EPSCs from all cells tested before and after puff. First EPSC: significant inhibition (Wilcoxon matched-pairs signed rank test, n = 6 individual cells, p = 0.031); second EPSC: significant inhibition (Wilcoxon matched-pairs signed rank test, n = 6 individual cells, p = 0.031). **e-g**, Same protocol after addition of ARL67156. No significant change induced by 2-AG. (Wilcoxon

matched-pairs signed rank test, n = 6 individual cells; first EPSC, p = 0.06; second EPSC, p = 0.06). **d**, Degree of inhibition of first EPSC. Significant difference (Wilcoxon matched-pairs signed rank test, n = 6 individual cells, p = 0.031). **h**, PPR before and after 2-AG in control conditions and after ARL67156. Significant increase in control (Wilcoxon matched-pairs signed rank test, n = 6 individual cells, p = 0.03). No significant change after ARL67156 (Wilcoxon matched-pairs signed rank test, n = 6 individual cells, p = 0.99). **i-p**, Same protocol. **k**, First EPSC: significant inhibition (Wilcoxon matched-pairs signed rank test, n = 6 individual cells, p = 0.03); second EPSC, no significant difference (Wilcoxon matched-pairs signed rank test, n = 6 individual cells, p = 0.41). **n**, After DPCPX, no significant inhibition (Wilcoxon matched-pairs signed rank test, n = 6; first EPSC, p = 0.31; second EPSC, p = 0.22). **o**, Significant inhibition (Wilcoxon matched-pairs signed rank test, n = 6 individual cells, p = 0.031). **p**, PPR before and after depolarization in control conditions and after DPCPX. Significant increase in control (Wilcoxon matched-pairs signed rank test, n = 6 individual cells, p = 0.031). No significant change after DPCPX (p = 0.99). **q-s**, Same protocol as in Fig. 3a-c. **s**, Mean EPSC amplitudes before and after depolarization. First EPSC: significant inhibition (Wilcoxon matched-pairs signed rank test, n = 6 individual cells, p = 0.031); second EPSC: no significant difference (Wilcoxon matched-pairs signed rank test, n = 6 individual cells, p = 0.31). **u-w**, Same protocol after addition of DPCPX (5 μM) (purple). No significant change induced by depolarization (Wilcoxon matched-pairs signed rank test, n = 6 individual cells; first EPSC, p = 0.06; second EPSC, p = 0.06). **t**, Degree of inhibition of first EPSCs. Significant difference (Wilcoxon matched-pairs signed rank test, n = 6 individual cells, p = 0.03). **x**, PPR before and after depolarization in control conditions and after DPCPX. Significant increase in control (Wilcoxon matched-pairs signed rank test, n = 6 individual cells, p = 0.03). No significant change in DPCPX (Wilcoxon matched-pairs signed rank test, n = 6 individual cells, p = 0.69). Data are presented as mean values +/- SD. The statistical test used was two-sided.

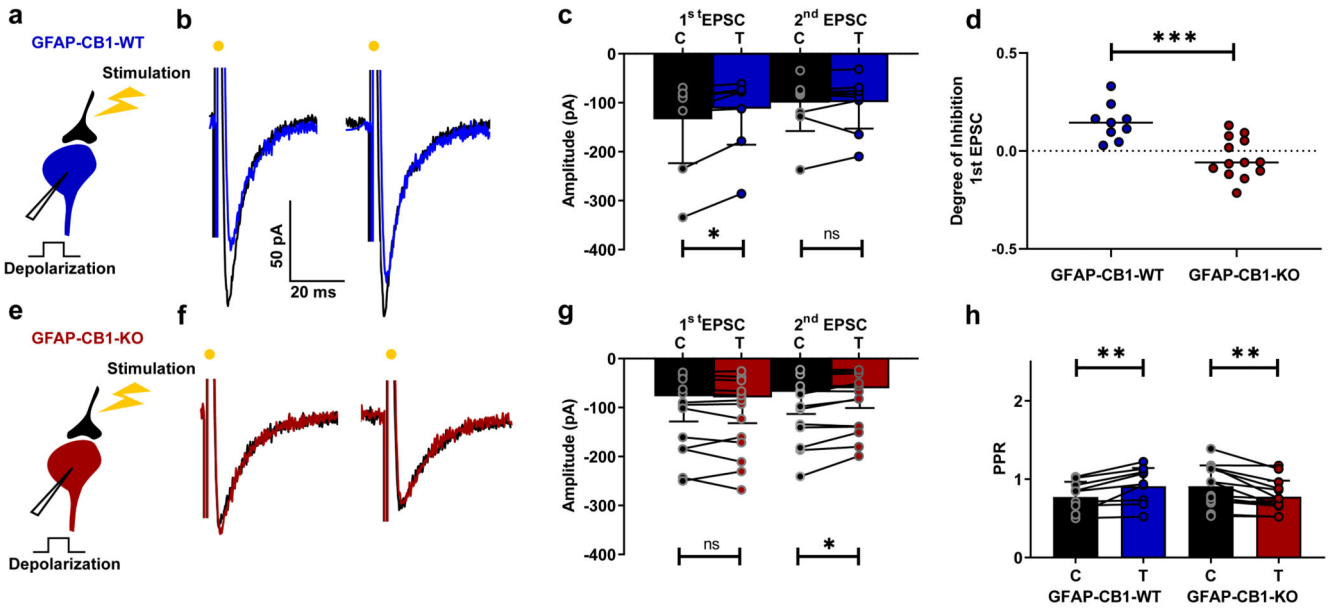

Fig. 7. DSE occurs in the adult spinal cord but not in animals lacking astrocytic CB1 receptors.

a, **e**, Schematic of spinal cord slice recording. **b**, Example average response (10 sweeps) of an interneuron to electric stimulation of excitatory axons before (black) and after a depolarizing pulse (blue) in a slice from a GFAP-CB1-WT mouse (P54). **c**, Mean EPSC amplitudes from all cells tested before and after depolarization. First EPSC: significant inhibition (p = 0.004, Wilcoxon matched-pairs signed rank test, n = 9 cells from 4 animals); second EPSC: no significant difference (p = 0.82, Wilcoxon matched-pairs signed rank test, n = 9 cells from 4 animals). **e-g**, Same protocol in a slice from GFAP-CB1-KO mouse (P53). No significant change of the first EPSC induced by depolarization (Wilcoxon matched-pairs signed rank test, n = 13 cells from 4 animals; first EPSC, p = 0.31; second EPSC, p = 0.02). **d**, Degree of inhibition of first EPSC. Significant difference (Mann-Whitney test, p = 0.0006). **h**, PPR before and after depolarization in GFAP-CB1-WT and GFAP-CB1-KO slices. Significant increase in GFAP-CB1-WT (Wilcoxon matched-pairs signed rank test, n = 9 cells from 4 animals, p = 0.004). Significant decrease in GFAP-CB1-KO (Wilcoxon matched-pairs signed rank test, n = 13 cells from 4 animals, p = 0.001). Data are presented as mean values +/- SD. The statistical tests used were two-sided.

Europe PMC Funders Author Manuscripts

Europe PMC Funders Author Manuscripts

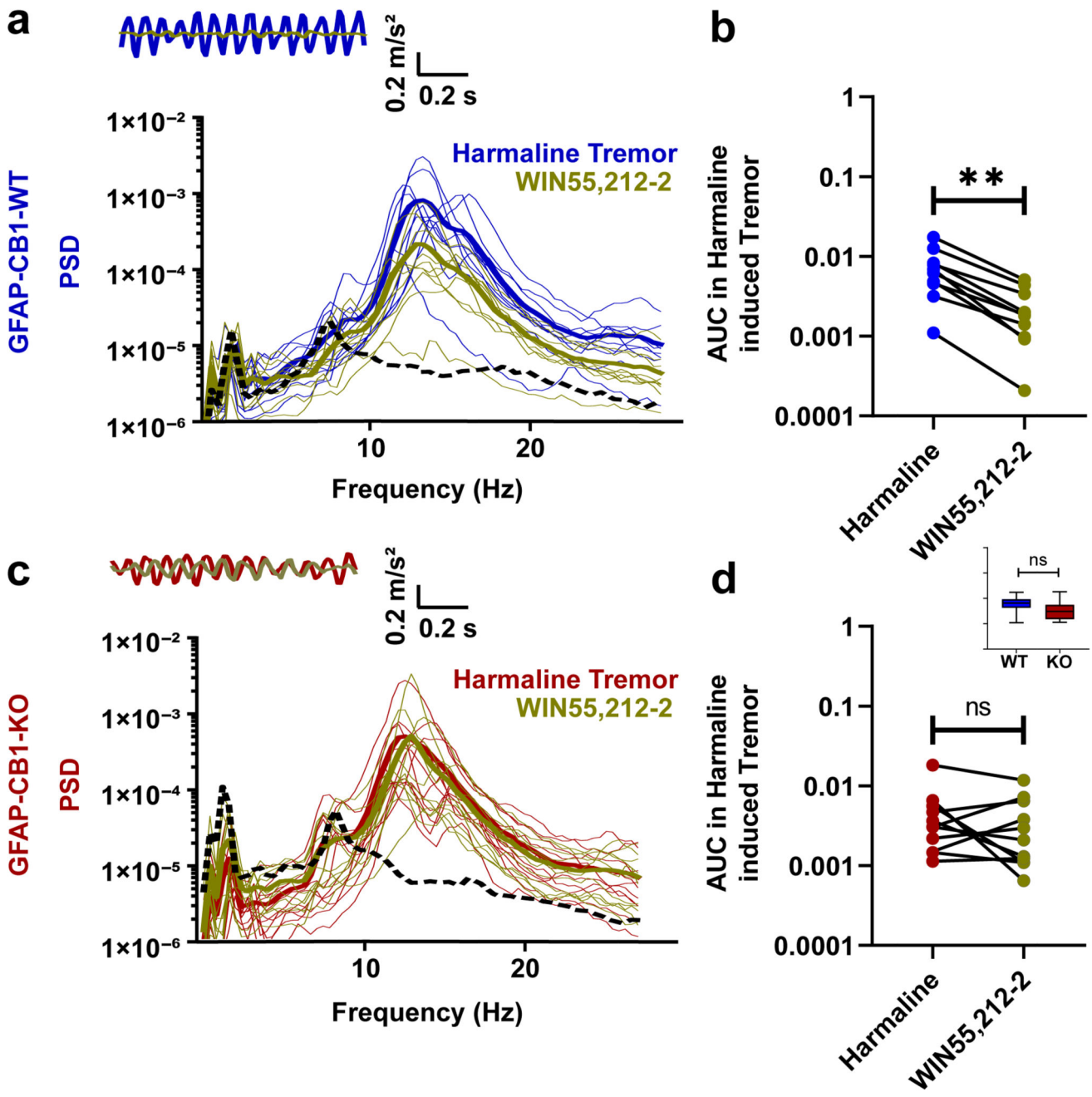

Fig. 8. Knocking out astrocytic CB_1 receptors prevents the anti-tremor effect of WIN55,212-2

a,c, Top: accelerometer traces. Bottom: power spectra of whole animal tremor. Dotted lines: examples of spontaneous tremor occurring before harmaline treatment. **a**, Raw trace recorded by the accelerometer for a GFAP-CB1-WT mouse before (blue) and after intrathecal injection of WIN55,212-2 (30mg/ml) (olive) and power spectra of tremor for all animals before and after injection of WIN55,212-2. **b**, Area under the curve (AUC) of the power spectra between 8Hz-25Hz. Significantly decrease after WIN55,212-2 intrathecal injection in GFAP-CB1-WT animals (Wilcoxon matched-pairs signed rank test, n = 10

animals, p = 0.002). **c**, Raw trace recorded by the accelerometer for a GFAP-CB1-KO mouse before (red) and after intrathecal injection of WIN55,212-2 (30mg/ml) (olive) and power spectra of tremor for all GFAP-CB1-KO animals before and after injection of WIN55,212-2. **d**, AUC of the power spectra between 8Hz-25Hz. Control AUC not significantly changed after intrathecal injection of WIN55,212-2 in GFAP-CB1-KO mice (Wilcoxon matched-pairs signed rank test, n = 11 animals, p = 0.41). Inset: Comparison of tremor induced between the two genotypes. Same scale as in b and d. No significant difference (Mann Whitney test, p = 0.08). Boxplot: Whiskers: minimum to maximum. Central lines: median. Bottom and top edges: 25th to 75th percentiles. The statistical tests used were two-sided.

Europe PMC Funders Author Manuscripts